Available online at www.sciencedirect.com
SCIENCE DIRECT®
International Journal of Heat and Mass Transfer 48 (2005) 4215–4228
International Journal of HEAT and MASS TRANSFER
www.elsevier.com/locate/ijhmt

New approaches to numerical modelling of droplet transient heating and evaporation

S.S. Sazhin [a,*], W.A. Abdelghaffar [a], P.A. Krutitskii [b], E.M. Sazhina [a], M.R. Heikal [a]

[a] School of Engineering, Faculty of Science and Engineering, University of Brighton, Cockcroft Building, Brighton BN2 4GJ, UK
[b] Faculty of Physics, Moscow State University, Vorobyovy gory, Moscow 119899, Russia

Received 1 October 2004
Available online 27 June 2005

Abstract

New approaches to numerical modelling of droplet heating and evaporation by convection and radiation from the surrounding hot gas are suggested. The finite thermal conductivity of droplets and recirculation in them are taken into account. These approaches are based on the incorporation of new analytical solutions of the heat conduction equation inside the droplets (constant or almost constant h) or replacement of the numerical solution of this equation by the numerical solution of the integral equation (arbitrary h). It is shown that the solution based on the assumption of constant convective heat transfer coefficient is the most computer efficient for implementation into numerical codes. This solution is applied to the first time step, using the initial distribution of temperature inside the droplet. The results of the analytical solution over this time step are used as the initial condition for the second time step etc. This approach is applied to the numerical modelling of fuel droplet heating and evaporation in conditions relevant to diesel engines, but without taking into account the effects of droplet break-up. It is shown to be more effective than the approach based on the numerical solution of the discretised heat conduction equation inside the droplet, and more accurate than the solution based on the parabolic temperature profile model. The relatively small contribution of thermal radiation to droplet heating and evaporation allows us to take it into account using a simplified model, which does not consider the variation of radiation absorption inside droplets.
© 2005 Elsevier Ltd. All rights reserved.

Keywords: Droplet heating; Conduction; Radiation; Evaporation; Diesel fuel

1. Introduction

Since the pioneering monograph by Spalding [1], the problem of modelling heating and evaporation of droplets has been widely discussed in Ref. [2–14]. In most practical engineering applications in CFD (Computational Fluid Dynamics) codes, however, only rather simplistic models for droplet heating have been used. These models have been based on the assumption that the thermal conductivity of liquid is infinitely high and the temperature gradients inside droplets can be ignored (see e.g. [15–17]). This simplification of the model was required due to the fact that droplet heating and

* Corresponding author. Tel.: +44 (0)1273 642300; fax: +44 (0)1273 642301.
E-mail address: s.sazhin@brighton.ac.uk (S.S. Sazhin).

0017-9310/$ - see front matter © 2005 Elsevier Ltd. All rights reserved.
doi:10.1016/j.ijheatmasstransfer.2005.04.007

Nomenclature

a	coefficient introduced in Eq. (21)
a_f	coefficient introduced in Eq. (10)
a_λ	liquid fuel absorption coefficient
b	coefficient introduced in Eq. (21)
b_f	coefficient introduced in Eq. (10)
B	coefficient introduced in Appendix A
B_λ	Planck function
B_M	Spalding mass number
c	specific heat capacity or molar concentration
$C_{1,2}$	coefficients in the Planck function
D_c	binary diffusion coefficient
f_n	coefficients introduced in formula (13)
$G(t,r)$	kernel defined by formula (13)
h	convection heat transfer coefficient
h_0	$\frac{hR_d}{k_l} - 1$
h_1	parameter introduced in formula (14)
$H(t)$	$\frac{h(t)R_d}{k_l} - 1$
k	thermal conductivity
L	specific heat of evaporation
Le	Lewis number
m	mass
M	molar mass
$M(t)$	$h(t)T_{eff}(t)R_d/k_l$
n	index of refraction
q_n	coefficients introduced in formula (11)
Q_a	efficiency factor of absorption
p	pressure
p_n	coefficients introduced in formula (11)
$P_1(R)$	power generated in unit volume
Pe	Peclet number
Pr	Prandtl number
r	normalised radius (R/R_d)
R	radius
Re	Reynolds number
t	time
T	temperature
$\widetilde{T}_0(r)$	variable introduced in formula (11)
$u(1,t)$	function introduced in formula (15)
$U(r,t)$	function introduced in formula (13)
$v_n(r)$	eigen functions used in Eq. (11)
$\|\|v_n(r)\|\|$	parameter introduced in Eq. (11)
w	normalized absorbed spectral power of radiation per unit volume
Y	mass fraction

Greek symbols

β_n	parameter introduced in Eq. (B1)
$\overline{\gamma}$	parameter introduced in Eq. (4)
γ_n	parameter introduced in Eq. (A2)
Δt	time step
ϵ	small parameter introduced in formula (13)
$\eta(t)$	parameter introduced in formula (13)
$\zeta(t)$	parameter introduced in formula (18)
κ	$k_l/(c_l\rho_l R_d^2)$
κ_λ	index of absorption
λ	wavelength
λ_n	eigen values used in formula (11)
$\mu_0(t)$	$\frac{hT_{eff}(t)R_d}{k_l}$
μ_c	parameter introduced in Eq. (4)
μ_*	parameter introduced in Eq. (4)
$\nu_0(t)$	function introduced in formula (13)
ξ	parameter introduced in formula (5)
ρ	density
τ	optical thickness or the argument in the integrands
τ_0	$a_\lambda R_d$
φ	parameter introduced in formula (A4)
ψ	parameter introduced in formula (18)

Subscripts

a	air
c	centre
d	droplet
eff	effective
ext	external
f	fuel
fs	saturated fuel vapour
g	gas
l	liquid
p	constant pressure
s	surface

evaporation had to be modelled alongside the effects of turbulence, combustion, droplet break-up and related phenomena in realistic 3D enclosures. Hence, finding a compromise between the complexity of the models and their computational efficiency is the essential precondition for successful modelling. Bertoli and Migliaccio [18] were perhaps the first who drew attention to the fact that the accuracy of CFD computations of heating, evaporation and combustion of diesel fuel sprays could be substantially increased if the assumption of infinitely high thermal conductivity of liquid is relaxed. They suggested that the numerical solution of the heat conduction equation inside the droplets is added to the solution of other equations in a CFD code. Although

this approach is expected to increase the accuracy of CFD predictions, the additional computational cost might be too high for practical applications.

An alternative approach to taking into account the effects of finite thermal conductivity and recirculation inside droplets have been suggested in [19]. This model is based on the parabolic approximation of the temperature profiles inside the droplets. This approximation does not satisfy the heat conduction equation with appropriate boundary conditions, but satisfies the equation of thermal balance at the droplet surfaces. Comparison with numerical solutions of the transient problem for moving droplets shows the applicability of this approximation to modelling the heating and evaporation processes of fuel droplets in diesel engines. The simplicity of the model makes it particularly convenient for implementation into multidimensional CFD codes to replace the above mentioned model of isothermal droplets. Preliminary results of the implementation of the simplified version of this model into a research version of the CFD code VECTIS of Ricardo Consulting Engineers have been demonstrated in [20].

Instead of solving numerically the heat conduction equation inside a droplet, or using a simplified model based on the parabolic approximation, one could think about the development of a numerical code based on the analytical solutions of this equation for the liquid finite thermal conductivity. A number of analytical solutions for a spherically symmetric problem have been obtained and discussed in [21–25]. In most cases these analytical solutions have been presented in the form of converging series.

The liquid finite thermal conductivity models (based on numerical or analytical solutions of the spherically symmetrical heat conduction equation) could be generalised to take into account the internal recirculation inside droplets. This could be achieved by replacing the thermal conductivity of liquid k_l by the so called effective thermal conductivity $k_{eff} = \chi k_l$, where the coefficient χ varies from about 1 (at droplet Peclet number $Pe_d = Re_d Pr_d < 10$) to 2.72 (at $Pe_d > 500$). It can be approximated as [5]:

$$\chi = 1.86 + 0.86 \tanh[2.225 \log_{10}(Pe_d/30)].$$

The values of transport coefficients in Pe_d are taken for liquid fuel, the relative velocity of droplets and their diameters are taken for calculation of Re_d. This model can predict the droplet average surface temperature, but not the distribution of temperature inside droplets. In our case, however, we are primarily interested in the accurate prediction of the former temperature, which controls droplet evaporation. Hence, the applicability of this model can be justified.

Some preliminary results of the implementation of the analytical solution obtained in [25] into a numerical code were reported in [26]. In [27] the effects of finite thermal conductivity of fuel droplets and external radiation on droplet evaporation and ignition of fuel vapour/air mixture were studied in detail based on a one dimensional code. In this code an analytical solution of the heat conduction equation in the presence of radiation was incorporated; this solution was coupled with the relevant equations for gas. A semi-analytical model for droplet evaporation reported in [28] is rather similar to that reported in [26], although the effects of thermal radiation were not taken into account, and a simplified form of the analytical solution was used. The problem of modelling the heating and evaporation of droplets, taking into account the effect of liquid finite thermal conductivity, is closely linked with the problem of modelling the heating and evaporation of multicomponent droplets (e.g. [9,29]). It is anticipated that some ideas developed in [26–28] and the present paper could be generalised to take into account the effects of multicomponent droplets, although the discussion of these possible generalisations is beyond the scope of this paper.

This paper is essentially an extended and updated version of the conference paper [26]. More specifically, the applicability of the results of the analysis of [19,25] to the problem of numerical modelling of heating and evaporation of droplets in engineering CFD codes will be investigated. This will be achieved via the analysis of accuracy and computer efficiency of various algorithms. The algorithms suggested can be easily implemented into any CFD code. The description of the details of this implementation, however, and the analysis of coupled solutions of the equations for liquid and gas phases are beyond the scope of this paper. This is done in our parallel paper [27]. In contrast to [28], both convective and radiative heating will be taken into account.

The basic equations and approximations used in our analysis are discussed in Section 2. Summary of the analytical solutions of the heat conduction equation is presented in Section 3. In Section 4 the numerical algorithms for incorporation of various models into CFD codes are discussed. The comparative analysis of these algorithms is given in Section 5. The main results of the paper are briefly summarised in Section 6.

2. Basic equations and approximations

Assuming that droplet heating is spherically symmetric, the transient heat conduction equation inside this droplet can be written as [21,22,25]:

$$c_l \rho_l \frac{\partial T}{\partial t} = k_l \left(\frac{\partial^2 T}{\partial R^2} + \frac{2}{R} \frac{\partial T}{\partial R} \right) + P_1(R), \quad (1)$$

where c_l is the liquid specific heat capacity, ρ_l and k_l are the liquid density and thermal conductivity respectively, $T = T(R,t)$ is the droplet temperature, R is the distance from the centre of the droplet, t is time and $P_1(R)$ is

the power generated in unit volume inside the droplet due to external radiation. c_l, ρ_l and k_l are assumed to be constant for the analytical solution of Eq. (1). Their variations with temperature and time will be accounted for when our analytical solutions are incorporated into the numerical code. This will be discussed later in Sections 4 and 5.

Assuming that the droplet is heated by convection from the surrounding gas, and cooled down due to evaporation, the energy balance equation at the droplet surface can be written as:

$$h(T_g - T_s) = -\rho_l L \dot{R}_d + k_l \left.\frac{\partial T}{\partial R}\right|_{R=R_d}, \tag{2}$$

where $h = h(t)$ is the convection heat transfer coefficient (time dependent in the general case), R_d is the droplet's radius, T_g is the gas ambient temperature, T_s is the droplet's surface temperature, L is the specific heat of evaporation. We took into account that $\dot{R}_d < 0$. Eq. (2) can be considered as a boundary condition for Eq. (1) at $R = R_d$. This needs to be complemented by the boundary condition at $R = 0$:

$$\left.\frac{\partial T}{\partial R}\right|_{R=0} = 0.$$

The initial condition is taken in the form: $T(t = 0) = T_0(R)$.

The radiation term is presented as [30,31]:

$$P_l(R) = \frac{3\pi}{R_d}\int_{\lambda_1}^{\lambda_2} w(r,\lambda) Q_a B_\lambda(T_{ext})\,d\lambda, \tag{3}$$

where $r = R/R_d$, $B_\lambda(T_{ext})$ is the Planck function defined as:

$$B_\lambda(T_{ext}) = \frac{C_1}{\pi\lambda^5[\exp(C_2/(\lambda T_{ext})) - 1]},$$

$$C_1 = 3.742 \times 10^8 \ \frac{W\mu m^4}{m^2}, \quad C_2 = 1.439 \times 10^4 \ \mu m K,$$

λ is the wavelength in μm. T_{ext} is is the external temperature responsible for radiative heating which is assumed to be constant. Q_a is the efficiency factor of absorption. The required approximation for Q_a depends on the specific application of the model. If this application is focused on the problem of heating and evaporation of diesel fuel droplets it can be estimated as [30,31]:

$$Q_a = \frac{4n}{(n+1)^2}[1 - \exp(-2a_\lambda R_d)],$$

where a_λ is the liquid fuel absorption coefficient, n is the refractive index of liquid diesel fuel; a_λ is related to the index of absorption κ_λ as $\kappa_\lambda = a_\lambda\lambda/(4\pi)$. $w(r,\lambda)$ is the normalised spectral power of radiation per unit volume absorbed inside the droplet. The following equations are used for the estimate of this power [31]:

$$w(r,\lambda) = \frac{[1 - \mu_* \Theta(r - 1/n)](r^2 + \bar{\gamma})}{[0.6(1-\mu_c^5) - \mu_c^3/n^2] + \bar{\gamma}(1-\mu_c^3)}, \tag{4}$$

where

$$\bar{\gamma} = (1.5/\tau_0^2) - (0.6/n^2),$$

$$\mu_* = \sqrt{1 - \left(\frac{1}{nr}\right)^2},$$

$$\mu_c = \sqrt{1 - \left(\frac{1}{n}\right)^2},$$

$$\tau_0 = a_\lambda R_d = 4\pi\kappa R_d/\lambda,$$

$$\Theta(x) = \begin{cases} 0 & \text{when } x < 0, \\ 1 & \text{when } x \geqslant 0 \end{cases}$$

or

$$w(\tau) = \frac{\xi^2\tau_0^3}{3}\frac{\exp[-\xi(\tau_0 - \tau)]}{\tau_0(\xi\tau_0 - 2) + (2/\xi)[1 - \exp(-\xi\tau_0)]}, \tag{5}$$

where $\tau = a_\lambda R$, $\xi = 2/(1 + \mu_c)$. Eq. (4) was used when $\tau_0 < n\sqrt{2.5}$, otherwise Eq. (5) was used. λ_1 and λ_2 describe the spectral range of thermal radiation which contributes to droplet heating. An alternative expression for w was obtained recently in [32]. Application of the expression given in [32] instead of the one given by Eqs. (4) and (5) is not expected to lead to any noticeable difference in the results.

Eq. (2) can be rearranged to:

$$T_{eff} - T_s = \frac{k_l}{hR_d}\left.\frac{\partial T}{\partial r}\right|_{r=1}, \tag{6}$$

where

$$T_{eff} = T_g + \frac{\rho_l L \dot{R}_d}{h}. \tag{7}$$

Eq. (6) is complemented by the boundary condition at $R = 0$ and the corresponding initial condition mentioned above.

The value of $\dot{R}_d$ is controlled by fuel vapour diffusion from the droplet surface. For stationary droplets it can be found from the equation [9]:

$$\frac{dm_d}{dt} = -4\pi\rho_g D_c R_d \ln(1 + B_M), \tag{8}$$

where m_d is the droplet mass, ρ_g is gas density, D_c is the binary diffusion coefficient, $B_M = Y_{fs}/(1 - Y_{fs})$ is the Spalding number, Y_{fs} is the mass fraction of fuel vapour near the droplet surface:

$$Y_{fs} = \left[1 + \left(\frac{p}{p_{fs}} - 1\right)\frac{M_a}{M_f}\right]^{-1}, \tag{9}$$

p and p_{fs} are ambient pressure and the pressure of saturated fuel vapour near the surface of droplets respectively, M_a and M_f are molar masses of air and fuel; p_{fs} can be calculated from the Clausius–Clapeyron equation presented in the form [33,4]:

$$p_{\rm fs} = \exp\left[a_{\rm f} - \frac{b_{\rm f}}{T_{\rm s} - 43}\right], \tag{10}$$

$a_{\rm f}$ and $b_{\rm f}$ are constants to be specified for specific fuels, $T_{\rm s}$ is the surface temperature of fuel droplets in K; $p_{\rm fs}$ predicted by Eq. (10) is in kPa. The quantity $\rho_{\rm g} D_{\rm c}$ in Eq. (8) can be replaced by $k_{\rm g}/c_{\rm pg}$ assuming that the Lewis number is unity ($Le = k_{\rm g}/(\rho_{\rm g} c_{\rm pg} D_{\rm c}) = 1$).

The generalisation of Eq. (8) to the case of moving droplets is well known [5]. However, since we are primarily interested in testing the new model for heating rather than evaporation of droplets, this generalisation is not important for our analysis, even if the effect of droplet motion on the value of the convective heat transfer coefficient is taken into account.

Eqs. (1) and (8) for droplets are complemented by the equations for droplet trajectory, the temperature of the gas phase ($T_{\rm g}$) and molar concentration of fuel vapour ($c_{\rm f}$) within the Lagrangian spray model. This system of ODEs of the Lagrangian model equations is coupled with the solution of PDEs of the Eulerian gas model. This is the conventional way of modelling spray/gas interaction in a CFD framework [15,16]. The focus of this paper, however, will be just on Eqs. (1) and (8). The analysis of coupled solutions is given in our parallel paper [27]. The evaporation model used in our analysis is similar to the one used in most CFD codes. It is based on the assumption that fuel vapour in the vicinity of fuel droplet surface is always saturated. More rigorous analysis of droplet evaporation would require a kinetic approach which is beyond the scope of this paper (see [34–37]).

3. Summary of analytical solutions

3.1. Case $h(t)$ = const.

In the case when $h(t)$ = const., the solution of Eq. (1) with $R_{\rm d}$ = const. and the corresponding boundary and initial conditions, as discussed in Section 2, can be presented as [25]:

$$T(r,t) = \frac{1}{r}\sum_{n=1}^{\infty}\left\{\frac{p_n}{\kappa\lambda_n^2} + \exp[-\kappa\lambda_n^2 t]\left(q_n - \frac{p_n}{\kappa\lambda_n^2}\right) - \frac{\sin\lambda_n}{\|v_n\|^2\lambda_n^2}\mu_0(0)\exp\left[-\kappa\lambda_n^2 t\right] - \frac{\sin\lambda_n}{\|v_n\|^2\lambda_n^2} \times \int_0^t \frac{{\rm d}\mu_0(\tau)}{{\rm d}\tau}\exp[-\kappa\lambda_n^2(t-\tau)]{\rm d}\tau\right\}\sin\lambda_n r + T_{\rm eff}(t), \tag{11}$$

where

$$\mu_0(t) = \frac{hT_{\rm eff}(t)R_{\rm d}}{k_{\rm l}}, \quad h_0 = (hR_{\rm d}/k_{\rm l}) - 1,$$

$$\|v_n\|^2 = \frac{1}{2}\left(1 + \frac{h_0}{h_0^2 + \lambda_n^2}\right), \quad \kappa = \frac{k_{\rm l}}{c_{\rm l}\rho_{\rm l}R_{\rm d}^2},$$

$$p_n = \frac{1}{\|v_n\|^2}\int_0^1 \tilde{P}(r)v_n(r){\rm d}r,$$

$$q_n = \frac{1}{\|v_n\|^2}\int_0^1 \tilde{T}_0(r)v_n(r){\rm d}r,$$

$$\tilde{P}(r) = rP(r), \quad \tilde{T}_0(r) = rT_0(R), \quad v_n(r) = \sin\lambda_n r \quad (n = 1, 2, \ldots),$$

a set of positive eigenvalues λ_n numbered in ascending order ($n = 1, 2, \ldots$) is found from the solution of the following equation:

$$\lambda\cos\lambda + h_0\sin\lambda = 0.$$

If $T_0(r)$ is twice differentiable, then the series in (11) converges absolutely and uniformly for all $t \geqslant 0$ and $r = R/R_{\rm d} \in [0,1]$.

In the limiting case when μ_0 = const., $P(r) = 0$, $\dot{R}_{\rm d} = 0$, $T_{\rm eff}$ = const. and $k_{\rm l} \to \infty$ Eq. (11) reduces to [24]:

$$T(t) \equiv T_{\rm d}(t) = T_{\rm s}(t) = T_{\rm g} + (T_{s0} - T_{\rm g})\exp\left(-\frac{3ht}{c_{\rm l}\rho_{\rm l}R_{\rm d}}\right). \tag{12}$$

Note that the value of $T(t) \equiv T_{\rm d}(t)$ does not depend on r. The same equation could be obtained directly from the energy balance equation at the surface of the droplet, assuming that there is no temperature gradient inside it.

3.2. Case of almost constant $h(t)$

Let us assume that [25]:

$$H(t) \equiv \frac{h(t)R_{\rm d}}{k_{\rm l}} - 1 = h_0 + \epsilon\eta(t),$$

where ϵ is a small parameter, and h_0 = const.

In this case the approximate solution of Eq. (1) can be written as [25]:

$$T(r,t) = \frac{1}{r}\left\{U(1,t) - \int_0^t M(\tau)G(t-\tau,1)\,{\rm d}\tau + \epsilon\int_0^t \eta(\tau)v_0(\tau)G(t-\tau,1)\,{\rm d}\tau\right\}, \tag{13}$$

where

$$U(r,t) = \sum_{n=1}^{\infty}\left\{\frac{p_n}{\kappa\lambda_n^2} + \exp[-\kappa\lambda_n^2 t]\left(q_n - \frac{p_n}{\kappa\lambda_n^2}\right)\right\}\sin(\lambda_n r),$$

$$G(t,r) = \kappa\sum_{n=1}^{\infty}\lambda_n^2 f_n \exp\left[-\kappa\lambda_n^2 t\right]\sin\lambda_n r = -\kappa\sum_{n=1}^{\infty}\frac{\sin\lambda_n}{\|v_n\|^2}\exp[-\kappa\lambda_n^2 t]\sin\lambda_n r,$$

$$M(t) = \frac{h(t)T_{\mathrm{eff}}(t)R_{\mathrm{d}}}{k_{\mathrm{l}}},$$

$$v_0(t) = U(1,t) - \int_0^t M(\tau)G(t-\tau,1)\mathrm{d}\tau.$$

$$f_n = -\frac{\sin\lambda_n}{\|v_n\|^2\lambda_n^2}.$$

3.3. Case $h(t) \neq$ const. (general case)

Let us assume that:

$$H(t) = h_0 + h_1(t), \tag{14}$$

where $h_0 = \text{const.} \neq -1$ and $h_1(t)$ is an arbitrary function of time.

In this case the solution of Eq. (1) can be written as:

$$T(r,t) = \frac{1}{r}\left\{U(r,t) - \int_0^t [M(\tau) - h_1(\tau)u(1,\tau)]G(t-\tau,r)\mathrm{d}\tau\right\}, \tag{15}$$

where $u(1,t)$ is found from the solution of the following integral equation:

$$u(1,t) = U(1,t) - \int_0^t [M(\tau) - h_1(\tau)u(1,\tau)]G(t-\tau,1)\mathrm{d}\tau, \tag{16}$$

and $U(1,t)$ is the same as in Eq. (13).

Eq. (16) is the Volterra integral equation of the second kind. It has a unique solution, although this solution cannot be found in an explicit form. The numerical scheme for its solution is described in [25].

3.4. A parabolic temperature profile model

Solution (11) can be reasonably accurately approximated by a parabolic function of r [19]:

$$T(r,t) = T_{\mathrm{c}}(t) + [T_{\mathrm{s}}(t) - T_{\mathrm{c}}(t)]r^2, \tag{17}$$

where T_{c} is the temperature in the centre of the droplet. This presentation of $T(r,t)$ takes into account the difference between the temperatures in the centre and at the surface of the droplet. The boundary condition at $R = 0$ is satisfied. The boundary condition at $R = R_{\mathrm{d}}$ and the condition for the thermal balance of the droplet leads to the following equation [19]:

$$T_{\mathrm{s}} = (\overline{T} + 0.2\zeta T_{\mathrm{g}})/\psi + 0.2\zeta\rho_{\mathrm{l}}R_{\mathrm{d}}\dot{R}_{\mathrm{d}}(T_{\mathrm{s}})L/(k_{\mathrm{l}}\psi). \tag{18}$$

where $\psi = 1 + 0.2\zeta$, $\zeta = 0.5Nuk_{\mathrm{g}}/k_{\mathrm{l}}$, $Nu = 2hR_{\mathrm{d}}/k_{\mathrm{g}}$ is the Nusselt number,

$$\overline{T} = \frac{3}{R_{\mathrm{d}}^3}\int_0^{R_{\mathrm{d}}} R^2T(R)\mathrm{d}R \tag{19}$$

is the average droplet temperature.

One of the main limitations of Eq. (18) is that it does not predict that $T_{\mathrm{s}}(t=0) = \overline{T}(t=0)$. This can be overcome by introducing the relevant corrections for small t [19]. These corrections, however, turned out to be not very important in most practical applications and will not be considered in this paper. Note that the parabolic model can be developed more rigorously based on Eq. (11) if only the first term in this series is taken into account, the contribution of thermal radiation is ignored and the initial temperature inside droplets is assumed to be constant. This approach was suggested in [38]. In the limit $t \to \infty$ Eq. (18) derived in [38] is identical with our Eq. (18) in the limit when $\dot{R}_{\mathrm{d}} = 0$. For $t \to 0$ the accuracy of Eq. (18) given in [38] becomes questionable since in this case all terms in Eq. (18) become comparable.

Results of further development of the parabolic temperature profile model taking into account the effect of evaporation are discussed in [39].

4. Numerical algorithms

We assume that the temperature of gas $T_{\mathrm{g}}(t)$ is given. The influence of droplets on it is ignored. This approximation would be justified in the case where the concentration of droplets of low. In realistic situations gas temperature can be calculated by the enthalpy transport equation with the source term describing the contribution of droplets. This is done in our parallel paper [27]. The values of the convection heat transfer coefficient depend on gas parameters (velocity and viscosity) alongside droplet radius. The latter is calculated using Eq. (8) and taking into account droplet swelling due to the decrease of liquid fuel density with increasing temperature. Under these assumptions the calculation of droplet temperature reduces to the solution of Eq. (1) subject to appropriate initial and boundary conditions. When calculating droplet radius we take into account the conservation of mass of liquid droplet during its swelling. This leads to the condition:

$$R_{\mathrm{d}}(\overline{T}) = R_{\mathrm{d}}(\overline{T}_{\mathrm{d0}})\left(\frac{\rho(\overline{T}_{\mathrm{d0}})}{\rho(\overline{T})}\right)^{1/3}, \tag{20}$$

where $\overline{T}$ is defined by Eq. (19).

In what follows, five numerical algorithms for the solution of the problem of droplet heating and evaporation will be considered. These will be based on the numerical solution of discretised heat conduction equation (1) and the solutions discussed in Sections 3.1–3.4.

4.1. Numerical solution of discretised equation (1)

There are various schemes for the numerical solution of discretised Eq. (1) widely discussed in CFD literature [40–42]. We use the fully implicit finite volume scheme.

4.2. Numerical algorithm using the solution for $h(t) = const.$

If the time step over which droplet temperature and radius are calculated is small, we can assume that $h(t) = \text{const}$. over this time. In this case we calculate $\dot{R}_d(t = 0)$ from Eq. (8) and $T_{eff}(t = 0)$ from Eq. (7). Then the initial condition at $t = 0$ will allow us to calculate $T(R, t)$ at the end of the first time step ($T(R, t_1)$) using Eq. (11). $R_d(t_1)$ is calculated based on Eq. (8) with the correction for swelling of the droplet (see Eq. (20)).

The same procedure is repeated for all the following time steps until the droplet is evaporated. The number of terms in the series in Eq. (11) which needs to be taken into account depends on the timing of the start of droplet heating and the time when the value of droplet temperature is calculated. For parameters relevant to diesel engine environments, just three terms in the series can be used with possible errors of not more than about 1% [25].

Note that the integrals over r, used to estimate $\overline{T}$ and q_n, can be calculated analytically as described in Appendix A.

At the very initial stage of droplet heating, when the boundary layer around the droplet does not have time to be established, the description of droplet heating in terms of the convection heat transfer coefficient might be not adequate [43–47].

4.3. Numerical algorithm using the solution for almost constant $h(t)$

When the change of $h(t)$ over a time step is small but still needs to be taken into account then the analytical solution for almost constant $h(t)$ can be applied. The difficulty in the application of the analytical solution given in Section 3.2 is that the value of $\epsilon\eta(t)$ cannot be a priori established in the general case, and iterations are required. The general scheme for the solution in this case starts with the first step for the case when $h(t) = \text{const}$. Droplet radius is calculated taking into account droplet swelling and evaporation. If the relative gas-droplet velocity is low then $h(t_1) = k_g/R_d(t_1)$. In the case where this velocity needs to be taken into account then the exchange of momentum between droplets and gas needs to be considered [16]. At the next stage we assume that $h(t)$ is a linear function of t in the range $(0, t_1)$. This allows us to assume that $\eta(t) = t$ and calculate ϵ as $\epsilon \equiv \epsilon_1 = (h(t_1) - h_0)/t_1$, where ϵ_1 indicates the value of ϵ for the first iteration. Then we calculate all parameters used in Eq. (13) and find the value of $T(r, t_1)$ from this equation. The updated values of $R_d(t_1)$ and $h(t_1)$ are calculated similarly to the case of $h(t) = \text{const}$. The value of $h(t_1)$ is expected to be close to the one predicted by the analysis based on the assumption that $h(t) = \text{const}$. In the unlikely event if this is not the case a further iteration is needed. Based on our experience, the prediction of the second iteration is practically indistinguishable from the prediction of the first iteration for realistic diesel engine conditions.

When considering the next time step between t_1 and t_2 we assume that $\eta(t) = t$ (as at the previous step). Then we assume that $\epsilon = \epsilon_1$, that is the value of ϵ at the second time step is the same as at the first time step. After that the value of $T(r, t_2)$ is calculated based on Eq. (13) and using the values of $T(r, t_1)$ as the initial condition. As a result, the values of $h(t_2)$ and $\epsilon_2 = (h(t_2) - h(t_1))/(t_2 - t_1)$ are obtained. The calculations of $T(r, t_2)$ are repeated for $\epsilon = \epsilon_2$. The updated values of $R_d(t_2)$ and $h(t_2)$ are calculated similarly to the case of $h(t) = \text{const}$. The same procedure is repeated for all the following time steps until the droplet is evaporated.

4.4. Numerical algorithm for arbitrary $h(t)$

It is unlikely that the numerical algorithm for arbitrary $h(t)$ is used in CFD calculations. It can, however, be useful for calculating heating of slowly evaporating individual droplets in a prescribed gas flow. Using the prescribed functions h_0 and $h_1(t)$ Eq. (16) is solved numerically for $u(1, t)$, based on the algorithm described in [25]. In the case of fast moving droplets the values of h_0 and $h_1(t)$ are calculated from known values of the droplet radius, gas thermal conductivity and the calculated time dependence of droplet relative velocity. Then the values of $T(r, t)$ are obtained from Eq. (15) for $T_{eff} = T_g$. At the next stage the values of $\dot{R}_d$ are calculated from Eq. (8) and the updated value of T_{eff} is found. The change of R_d over the time of calculations should be small. Otherwise, the equations described in Section 3.3 are not applicable.

4.5. Numerical algorithm for the parabolic temperature profile model

Although the algorithms described in Sections 4.1–4.3 are likely to describe the heating of droplets more accurately compared with the the case where the temperature gradients inside droplets are ignored altogether, they might be CPU intensive. A reasonable compromise between accuracy and CPU time requirements can be achieved for the parabolic temperature profile model described in Section 3.4. The effect of thermal radiation is ignored at this stage. It can be included as a perturbation if required [48].

The application of this model starts with finding the average droplet temperature ($\overline{T}$) from Eq. (19). Then the value of T_s is calculated from Eq. (18) assuming that $\dot{R}_d = 0$. Using this value of T_s the updated value of $\dot{R}_d$ is obtained. Then this updated value of $\dot{R}_d$ allows a more accurate estimate of T_s.

Note that in this algorithm we do not need to take into account the differential radiation heating of droplets as described by the function $w(r,\lambda)$, as we are not interested in the details of temperature distribution inside droplets. Instead, the global heating of droplets needs to be accounted for as described in [49,20,50].

5. Comparative analysis

In this section the performance of the schemes discussed in Section 4 will be compared for the parameters relevant to diesel engines. The initial droplet radius taken is equal to 10 μm, and its initial temperature is equal to 300 K. The droplet swelling and the temperature dependence of k_l are taken into account: the latter decreased from 0.145 W/m K to 0.02 W/m K when the droplet temperature increased from 300 K to 725 K [51]. The effect of droplet break-up will not be taken into account, and this might lead to unrealistically long droplet lifetimes. It is, however, essential to separate the effects of droplet heating and evaporation from other processes to get a better insight into advantages and limitations of various algorithms. At first we consider the case when the contribution of thermal radiation is ignored. Then the contribution of thermal radiation is discussed.

5.1. Comparison of numerical algorithms without thermal radiation

It is assumed that the convection heat transfer coefficient h decreases from $1.377k_g/R_d$ to k_g/R_d over 1 ms. This can approximate the reduction of the droplet relative velocity from 0.45 m/s to zero–the situation relevant to diesel engines when air entrainment by a fuel spray is taken into account [52,53]. At first the numerical algorithms using the solution for h = const., almost constant h and arbitrary h were compared for the case of droplet heating without evaporation. Gas temperature was taken equal to 1000 K.

All three algorithms predict almost the same dependence of droplet surface temperature on time. From the point of view of computer efficiency, however, the algorithm using the analytical solution for h = const., has had clear advantages over other algorithms. The CPU time required by this algorithm has been more than an order of magnitude less than the CPU time required by the algorithms with transient h for comparable accuracy of the results. Three terms in the analytical solution have been taken by this algorithm. We expect that this would introduce an error of the solution less than 1% for the values of parameters under consideration except at the very initial stage of calculations, the contribution of which can be ignored in most practical applications (see [25] for details). For benchmarking we used the numerical algorithm based on the solution for h = const., keeping 25 terms (corresponding to 25 eigenvalues) in the series. This truncation of the series becomes more difficult in the case of the solution for almost constant and arbitrary h. In both these cases the solution is presented in integral forms (see Eqs. (13) and (16)). Truncation of the series in $G(t,r)$ would lead to substantial errors in evaluating $G(t,r)$ in the limit $t \to 0$. These, in their turn, are expected to lead to errors in calculating the integrals in Eqs. (13) and (16) regardless of the values of t. These results allow us to focus on the algorithm using the solution for h = const. for the implementation in CFD codes.

At the next stage we compared the performance of this algorithm with the performance of the numerical solution of the discretised heat conduction equation, the performance of the numerical algorithm based on the parabolic temperature profile model, and the numerical algorithm based on the assumption that there is no temperature gradient inside the droplet (Eq. (12)). As in the previous analysis we assumed that T_g = 1000 K, but allowed droplets to evaporate and swell.

Results of our calculations of the droplet surface temperature and radius as functions of time, using the above mentioned four algorithms, are shown in Fig. 1. As follows from this figure, the predictions of numerical calculations based on the numerical solution of the discretised heat conduction equation and the algorithms using the analytical solution for h = const. almost coin-

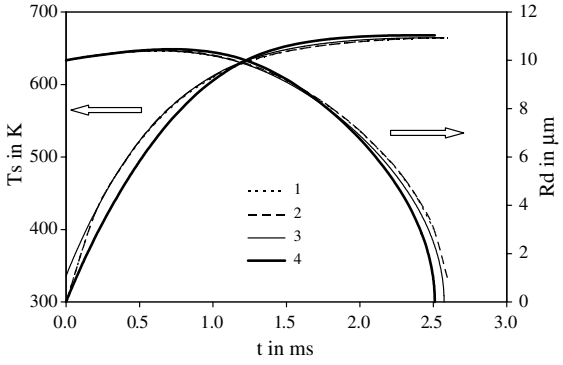

Fig. 1. Plots of droplet surface temperature T_s and radius R_d versus time, without taking into account the effect of thermal radiation. It is assumed that the convection heat transfer coefficient h decreases from $1.377k_g/R_d$ to k_g/R_d over 1 ms. Gas temperature is taken equal to 1000 K. The calculations have been performed using the numerical algorithms based on the analytical solution for h = const. (curves 1), direct numerical solution of the discretised heat conduction equation (curves 2), the numerical solution based on the parabolic temperature profile model (curves 3), and the numerical solution based on the assumption that there is no temperature gradient inside the droplet (curves 4). Curves 1 and 2 coincide within the accuracy of plotting.

cide for both the surface temperature and droplet radius. Both these solutions differ noticeably from the predictions of the model based on the assumption of no temperature gradient inside the droplet. The predictions of the parabolic model are between the above mentioned solutions. This means that from the point of view of potential accuracy, the numerical solution of the discretised heat transfer equation and the solution based on the algorithms using the solution for h = const. (keeping three terms in the series) are practically identical and superior to the numerical solutions based on the parabolic temperature profile model and the model with no temperature gradient inside the droplet. Accuracy, however, is not the only parameter which determines the applicability of the model for the implementation into CFD codes. Another parameter which needs to be accounted for is CPU requirement.

The plots of errors and CPU times versus time step Δt for the numerical algorithm based on the analytical solution for h = const. and numerical solution of the discretised heat conduction equation are shown in Fig. 2. 100 nodes along the radius were considered for the latter solution to provide calculations with relative errors of less than about 0.5%. The calculations for the parabolic temperature profile model and the numerical solution based on the assumption that there is no temperature gradient inside the droplet were performed using the adaptive time step. The errors of these calculations relative to the prediction of the numerical solution of the discretised heat conduction equation were 1.2% and 3.6% respectively. All errors were calculated relative to the prediction of the numerical solution of the discretised heat conduction equation with 1000 nodes along droplet radius and time step $\Delta t = 0.001$ ms. As follows from Fig. 2, the errors of calculations based on the algorithm using the analytical solution for h = const. are consistently lower when compared with the errors of calculations based on the numerical solution of the discretised heat transfer equation for $\Delta t > 0.01$ ms. At smaller Δt these errors are close to zero for both solutions. This can be related to the fact that the numerical solution of the discretised heat conduction equation is based on the assumption that non-linear terms can, with respect to the time step, be ignored, while the algorithms using the analytical solution for h = const. implicitly retain these terms.

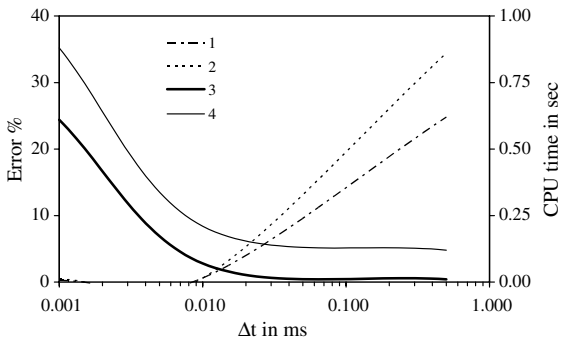

Fig. 2. Plots of errors and CPU times of calculation of evaporation time versus time step for the calculations presented in Fig. 1. The errors were calculated relative to the prediction of the numerical solution of the discretised heat conduction equation with $\Delta t = 10^{-6}$ s and using 1000 nodes along droplet radius. The plots of errors are presented for the numerical algorithm based on the analytical solution for h = const. (curves 1) and numerical solution of the discretised heat conduction equation (curves 2). Plots of CPU times are presented for the algorithm based on the analytical solution for h = const. (curves 3) and numerical solution of the discretised heat conduction equation (curves 4). The calculations for the parabolic temperature profile model and the numerical solution based on the assumption that there is no temperature gradient inside the droplet were performed using the adaptive time step. The errors of these calculations relative to the prediction of the direct numerical solution were 1.2% and 3.6% respectively.

As mentioned above, the errors of the numerical algorithm based on the parabolic temperature profile model are generally less than the errors of the numerical algorithm based on the assumption that there is no temperature gradient inside droplet. The CPU requirements of the parabolic temperature profile model, however, are slightly larger than those of the model based on the assumption of no temperature gradients inside droplets. In both cases, however, they are expected to be less than for more rigorous models for the same time step. It is recommended that the numerical algorithm based on the parabolic temperature profile model is used in CFD codes if the high accuracy of calculations is not essential. Note that the solution predicted by the algorithm using the analytical solution for h = const. reduces to that predicted by the numerical algorithm based on the assumption that there is no temperature gradient inside droplet in the limit when $k_l \to \infty$ (the value k_l = 10 W/m K was used for this calculation).

5.2. Comparison of numerical algorithms with thermal radiation

There can be two different approaches to modelling the effects of thermal radiation on heating and evaporation of droplets. If we intend to take into account the distribution of thermal radiation absorption inside droplets we first need to use the term $P_1(R)$ in Eq. (1) as defined by Eq. (3). If we ignore the distribution of thermal radiation absorption inside droplets then a much simpler approach can be used as suggested in [49,20,50]:

$$P_1(R) = 3 \times 10^6 a\sigma R_{\mathrm{d}(\mu\mathrm{m})}^{b-1}\theta_{\mathrm{R}}^4, \tag{21}$$

where θ_{R} is the radiation temperature (assumed equal to the external temperature), $R_{\mathrm{d}(\mu\mathrm{m})}$ is the droplet radius in

μm, a and b are polynomials of external temperature (quadratic functions in the first approximation). The expressions for these coefficients for a typical automotive diesel fuel (low sulphur ESSO AF1313 diesel fuel) in the range of external temperatures 1000–3000 K was used in our analysis [50]. Note that the assumption that θ_R is equal to the external temperature is valid in the case of optically thin gas. In the case of optically thick gas we can assume that θ_R is equal to the gas temperature in the vicinity of the droplet.

Expression (3) is certainly more accurate than Expression (21), but its application requires much more CPU time than application of Expression (21). Most of the CPU time is actually spent on calculation of the integral over λ in this expression. The most accurate calculation of this integral is based on all experimentally measured values of absorption coefficient a_λ (4111 points). As follows from our analysis, the reduction of the number of these point to just 58, allows us to reduce CPU time by almost two orders of magnitude with the introduction of an error of less than 10%. This error can be tolerated in most cases, and this approach is used in our paper. The analysis of [31] was based on the results of measurements of λ in the ranges 0.5–1.1 μm and 2.0–6.0 μm, while our results are based on the measurements in the range 0.2–6.0 μm. Note that when we use $P_1(R)$ in the form (21), the expression for p_n used in Eq. (11) can be simplified considerably (see Appendix B).

To illustrate the effect of thermal radiation on droplet heating and evaporation we consider modelling droplet heating and evaporation in the gas at the temperature 700 K near the droplet and external temperature of 2500 K (this temperature can be identified with the temperature of remote flame). These values of temperature are extreme rather than typical, but they are used to illustrate the effect of thermal radiation [54]. As we did in the previous section we took droplet radius equal to 10 μm and its initial temperature equal to 300 K. In contrast to the previous section we assumed that the convective heat transfer coefficient is equal to $k_g/R_d(t)$ throughout the droplet lifetime (this refers to stationary or almost stationary droplets relative to the surrounding gas). The problem has been solved in the following approximations:

(a) Temperature gradient inside the droplet, and contribution of radiation are not taken into account (Eq. (12)).
(b) Temperature gradient inside the droplet is not taken into account. The contribution of radiation is taken into account based on the presentation of P_1 in the form (21).
(c) No contribution of radiation, but the temperature gradient inside the droplet is taken into account. Numerical algorithm of the solution of Eq. (1) is based on the analytical solution corresponding to constant h (Eq. (11)), applied at each time step.
(d) The same as case (c) but with contribution of radiation taken into account based on the presentation of P_1 in the form (3).
(e) The same as case (c) but with contribution of radiation taken into account based on the presentation of P_1 in the form (21).
(f) The temperature gradient inside the droplet is taken into account. The numerical solution of the discretised equation (1) with the radiation term in the form (21) is performed using the finite volume technique with fully implicit marching in time.

In Fig. 3 the surface temperatures and radii of droplets predicted by the models based on approximations 'd' and 'e' are compared. The values of Δt were taken equal to 10^{-6} s. As can be seen from this figure, the time evolution of surface temperature predicted by both models practically coincide. The time evolution of droplet radii predicted by these models differ slightly, but this difference can be ignored in most practical applications. This result agrees with the one reported in [13,14], where the numerical solution of the heat transfer equation inside the droplet in the presence of convection, radiation and internal recirculation was performed. Note that the values of $P_1(R)$ obtained based on Eq. (3), already contained an error of about 10% (see the discussion above). Recall that the values of parameters used for our comparison are extreme rather than typical for the diesel engine environment. In more realistic cases this difference between the curves is expected to be even

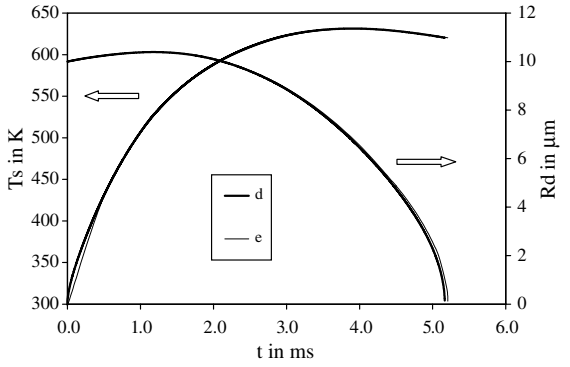

Fig. 3. Plots of droplet surface temperature T_s and radius R_d versus time taking into account the effects of thermal radiation. The convective heat transfer coefficient is assumed to be equal to $k_g/R_d(t)$ throughout the droplet lifetime. The letters 'd' and 'e' near the curves correspond to the numerical algorithms used as indicated in the text.

smaller. Under these circumstances, the application of the radiation term in the form (21) seems to have clear advantages when compared with the application of the radiation term in the form (3), due to simplicity of the former. This allows us to recommend the application of radiation term in the form (21) for practical calculations in CFD codes.

The plots of droplet surface temperature and radius predicted by the models based on approximations 'a'–'c' and 'e'–'f' is shown in Fig. 4. The values of Δt were taken as equal to 10^{-6} s and for the case 'f' ΔR were taken as equal to $R_d/100$ as in the case without radiation (the error introduced by this ΔR compared with the case when $\Delta R = R_d/1000$ was less than 0.5% for $\Delta t = 10^{-6}$ s). As can be seen from this figure, the effect of radiation tends to increase droplet evaporation due to the additional heat source, as expected. The effect of temperature gradient is expected to lead to an increase in droplet surface temperature when compared with the droplet average temperature. This would lead to an increase in droplet evaporation due to the direct temperature effect, and its decrease due to the decrease of convective heat supply to droplet surface. As follows from Fig. 4, the second effect dominates over the first, and the rate of droplet evaporation decreases. The curves b, e and f in Fig. 4 appear to be rather close to each other. This means that the predictions of the numerical algorithm of the solution of Eq. (1) based on the analytical solution corresponding to constant h and the numerical solution of the discretised equation with the radiation terms taken into account give rather similar results.

The errors in evaporation time as the functions of Δt for the cases 'c', 'e' and 'f' are shown in Fig. 5. The errors in all cases are calculated relative to the predictions of the numerical solution of the discretised heat conduction equation with $\Delta t = 10^{-6}$ s and $\Delta R = R_d/1000$. As can be seen from Fig. 5, the largest errors are those for the curve 'c' which corresponds to the case where the effect of radiation is not taken into account. Hence, radiation cannot be ignored in this case. The errors for other curves increase with increasing Δt. This error in the predicted evaporation times is negligibly small at $\Delta t < 10^{-5}$ s and can be tolerated in most practical applications.

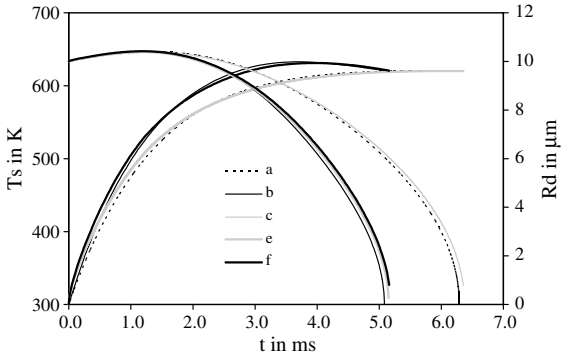

Fig. 4. The same as Fig. 3 but for numerical algorithms 'a'–'c' and 'e'–'f'.

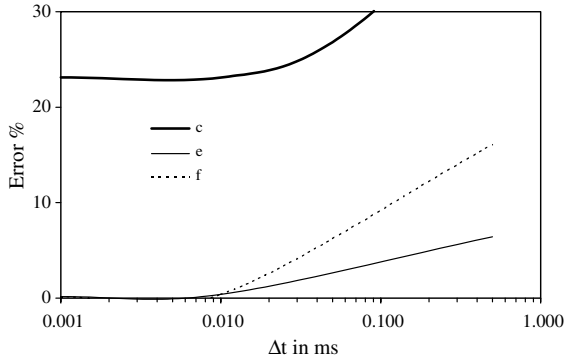

Fig. 5. Plots of errors of calculation of evaporation time versus time step for the curves 'c', 'e' and 'f' presented in Fig. 4. These errors were calculated relative to the prediction of the numerical solution of the discretised heat conduction equation with $\Delta t = 10^{-6}$ s and using 1000 divisions along droplet radius. The letters near the curves correspond to the numerical algorithms used as indicated in the text.

As follows from Fig. 6, the CPU requirements for the case 'd' are more than an order of magnitude larger than for other curves. This CPU requirement is difficult to justify in view of the very small improvement of the accuracy of calculations. Comparing curves 'e' and 'f' we can see that the CPU time for the algorithm based on the analytical solution is always much less than CPU time for algorithm based on the numerical solution of the discretised equation (1). This allows us to

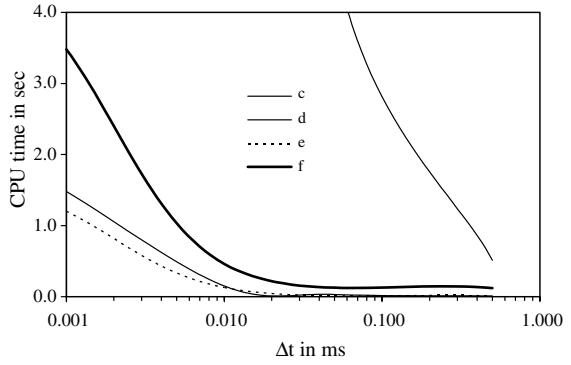

Fig. 6. Plots of CPU time versus time step for the curves 'c'–'f' presented in Figs. 3 and 4. The letters near the curves correspond to the numerical algorithms used as indicated in the text.

recommend the former algorithm with the radiation term in the form (21) for practical applications, including possible implementation into CFD codes.

Note that the CPU time required for the case without radiation (curve 'c') is slightly larger than for the case when the radiation is taken into account and the radiation term is taken in the form (21). This is related to the fact that in the case without radiation droplet needs longer time to evaporate.

6. Conclusions

Several new approaches to numerical modelling of droplet heating and evaporation by convection and radiation from the surrounding hot gas have been suggested. Finite thermal conductivity of the droplets and internal recirculation in them have been taken into account via the introduction of the effective thermal conductivity of the droplets k_{eff}. Gas temperature T_g and convective heat transfer coefficient h have been taken as arbitrary functions of time. The analytical solutions of the heat conduction equation inside the droplet have been presented for the cases when h is constant or almost constant. In the case when h is an arbitrary function of time, this solution is reduced to the solution of the Volterra integral equation of the second kind. Our approaches have been based on the incorporation of these solutions into a numerical code, when gas temperature and convection heat transfer coefficient vary with time. It has been shown that the solution based on the assumption of constant convective heat transfer coefficient is the most efficient for the implementation into numerical codes. Initially, this solution is applied at the first time step, using the initial distribution of temperature inside the droplet. The results of the analytical solution over this time step are used as the initial condition for the second time step etc. This approach has been compared with the approaches based on the numerical solution of the discretised heat conduction equation, those based on the assumption that there is no temperature gradient inside the droplet, and those based on the assumption that the temperature distribution inside the droplet has a parabolic profile. All these approaches have been applied to the numerical modelling of fuel droplet heating and evaporation in conditions relevant to diesel engines, but without taking into account the effects of droplet break-up. The algorithm based on the analytical solution for constant h has been shown to be more effective (from the points of view of the balance of accuracy and CPU time requirement) than the approach based on the numerical solution of the discretised heat conduction equation inside the droplet, and more accurate than the solution based on the parabolic temperature profile model. The relatively small contribution of thermal radiation to droplet heating and evaporation allows us to describe it using a simplified model, which takes into account their semi-transparency, but does not consider the spatial variations of radiation absorption inside droplets.

Acknowledgement

The authors are grateful to the EPSRC (grant GR/R82920/01) and the Royal Society for the financial support of this project.

Appendix A. Calculation of $\overline{T}$ and q_n in the numerical algorithm using the analytical solution for h = const.

Let us present Eq. (11) in the form:

$$T(r,t_n)=\frac{1}{r}\sum_{n'=1}^{\infty}\gamma_{n'(p)}\sin(\lambda_{n'(p)}r)+T_{\text{eff}}(t_n), \tag{A1}$$

where

$$\gamma_n=\frac{p_n}{\kappa\lambda_n^2}+\exp[-\kappa\lambda_n^2 t]\left(q_n-\frac{p_n}{\kappa\lambda_n^2}\right)-\frac{\sin\lambda_n}{\|v_n\|^2\lambda_n^2}\mu_0(0)\exp[-\kappa\lambda_n^2 t]-\frac{\sin\lambda_n}{\|v_n\|^2\lambda_n^2}\int_0^t\frac{\mathrm{d}\mu_0(\tau)}{\mathrm{d}\tau}\exp[-\kappa\lambda_n^2(t-\tau)]\mathrm{d}\tau, \tag{A2}$$

all parameters in Eq. (A2) are taken at the previous time step t_{n-1} (indicated by the additional subscript (p)).

Having substituted Eq. (A1) into Eq. (19) we obtain:

$$\overline{T}(t_n)=3\sum_{n'=1}^{\infty}\gamma_{n'(p)}\int_0^1 r\sin(\lambda_{n'(p)}r)\mathrm{d}r+3T_{\text{eff}}(t_n)\int_0^1 r^2\mathrm{d}r=3(1+h_0)\sum_{n'=1}^{\infty}\frac{\gamma_{n'(p)}\sin\lambda_{n'(p)}}{\lambda_{n'(p)}^2}+T_{\text{eff}}(t_n). \tag{A3}$$

Similarly, having substituted Eq. (A1) into the definition of q_n we obtain:

$$q_n(t_n)=\frac{1}{\|v_n\|^2}\sum_{n'=1}^{\infty}\gamma_{n'(p)}\int_0^1\sin(\lambda_{n'(p)}r)\sin(\lambda_n r)\mathrm{d}r+\frac{T_{\text{eff}}(t_n)}{\|v_n\|^2}\int_0^1 r\sin(\lambda_n r)\mathrm{d}r=\varphi_n+\frac{T_{\text{eff}}(t_n)(1+h_0)\sin\lambda_n}{\|v_n\|^2\lambda_n^2}, \tag{A4}$$

where

$$\varphi_n=\begin{cases}\gamma_n \quad \text{when } \lambda_{n(p)}=\lambda_n,\\ \dfrac{1}{2\|v_n\|^2}\displaystyle\sum_{n'=1}^{\infty}\gamma_{n'(p)}\left[\frac{\sin(\lambda_{n'(p)}-\lambda_n)}{\lambda_{n'(p)}-\lambda_n}-\frac{\sin(\lambda_{n'(p)}+\lambda_n)}{\lambda_{n'(p)}+\lambda_n}\right]\\ \quad \text{when } \lambda_{n(p)}\neq\lambda_n.\end{cases}$$

Appendix B. Expression for p_n for the simplified form of the radiation term

Assuming that $\theta_R = T_{ext}$ and ignoring the contribution of $\overline{T}$, substitution of $P_1(R)$, defined by Eq. (21) into the expression for p_n gives:

$$p_n = \frac{1}{\|v_n\|^2}\int_0^1 3\times 10^6 a\sigma R_{d(\mu m)}^{b-1} T_{ext}^4 r\sin(\lambda_n r)\mathrm{d}r = \frac{\beta_n}{\lambda_n^2}(1+h_0)\sin\lambda_n, \quad \text{(B1)}$$

where

$$\beta_n = \frac{3\times 10^6 a\sigma R_{d(\mu m)}^{b-1} T_{ext}^4}{\|v_n\|^2}.$$

References

[1] D.B. Spalding, Convective Mass Transfer, Edward Arnold Ltd, 1963.
[2] G.M. Faeth, Evaporation and combustion of sprays, Progr. Energy Combust. Sci. 9 (1983) 1–76.
[3] K.-K. Kuo, Principles of Combustion, John Wiley & Sons, 1986.
[4] A.H. Lefebvre, Atomization and Sprays, Taylor & Francis, 1989.
[5] B. Abramzon, W.A. Sirignano, Droplet vaporization model for spray combustion calculations, Int. J. Heat Mass Transfer 32 (1989) 1605–1618.
[6] S.K. Aggarwal, A review of spray ignition phenomena: present status and future research, Progr. Energy Combust. Sci. 24 (1998) 565–600.
[7] J.F. Griffiths, J.A. Barnard, Flame and Combustion, Blackie Academic & Professional, 1995.
[8] G.L. Borman, K.W. Ragland, Combustion Engineering, McGraw-Hill, 1998.
[9] W.A. Sirignano, Fluid Dynamics and Transport of Droplets and Sprays, Cambridge University Press, 1999.
[10] R.B. Bird, W.E. Stewart, E.N. Lightfoot, Transport Phenomena, John Wiley & Sons, 2002.
[11] A. Mukhopadhyay, D. Sanyal, A spherical cell model for multi-component droplet combustion in a dilute spray, Int. J. Energy Res. 25 (2001) 1275–1294.
[12] G. Miliauskas, Interaction of the transfer processes in semitransparent liquid droplets, Int. J. Heat Mass Transfer 46 (2003) 4119–4138.
[13] B. Abramzon, S. Sazhin, Droplet vaporization model in the presence of thermal radiation, Int. J. Heat Mass Transfer 48 (2005) 1868–1873.
[14] B. Abramzon, S. Sazhin, Convective vaporization of fuel droplets with thermal radiation absorption, Fuel, in press.
[15] S.S. Sazhin, G. Feng, M.R. Heikal, I. Goldfarb, V. Goldshtein, G. Kuzmenko, Thermal ignition analysis of a monodisperse spray with radiation, Combustion and Flame 124 (2001) 684–701.
[16] E.M. Sazhina, S.S. Sazhin, M.R. Heikal, V.I. Babushok, R.J.R. Johns, A detailed modelling of the spray ignition process in Diesel engines, Combustion Science and Technology 160 (2000) 317–344.
[17] S.V. Utyuzhnikov, Numerical modelling of combustion of fuel-droplet- vapour releases in the atmosphere, Flow, Turbulence and Combustion 68 (2002) 137–152.
[18] C. Bertoli, M. na Migliaccio, A finite conductivity model for diesel spray evaporation computations, Int. J. Heat Fluid Flow 20 (1999) 552–561.
[19] L.A. Dombrovsky, S.S. Sazhin, A parabolic temperature profile model for heating of droplets, ASME Journal of Heat Transfer 125 (2003) 535–537.
[20] S.S. Sazhin, L.A. Dombrovsky, P.A. Krutitskii, E.M. Sazhina, M.R. Heikal, Analytical and numerical modelling of convective and radiative heating of fuel droplets in diesel engines. Proceedings of the Twelfth International Heat Transfer Conference. Grenoble (August 18–23, 2002), vol. 1, Editions scientifique et medicale Elsevier SAS, 2002, pp. 699–704.
[21] H.S. Carslaw, J.C. Jaeger, Conduction of Heat in Solids, Clarendon Press, Oxford, 1986.
[22] A.V. Luikov, Analytical Heat Transfer Theory, Academic Press, 1968.
[23] E.M. Kartashov, Analytical Methods in the Heat Transfer Theory in Solids, Vysshaya Shkola, Moscow, 2001 (in Russian).
[24] S.S. Sazhin, P.A. Krutitskii, A conduction model for transient heating of fuel droplets, in: Progress in Analysis, in: H.G.W. Begehre, R.P. Gilbert, M.W. Wong (Eds.), Proceedings of the 3rd International ISAAC (International Society for Analysis, Applications and Computations) Congress (August 20–25, 2001, Berlin), vol. II, World Scientific, Singapore, 2003, pp. 1231–1239.
[25] S.S. Sazhin, P.A. Krutitskii, W.A. Abdelghaffar, E.M. Sazhina, S.V. Mikhalovsky, S.T. Meikle, M.R. Heikal, Transient heating of diesel fuel droplets, Int. J. Heat Mass Transfer 47 (2004) 3327–3340.
[26] S.S. Sazhin, P.A. Krutitskii, W.A. Abdelghaffar, E.M. Sazhina, M.R. Heikal, Transient heating of droplets, in: Proceedings of '3rd International Symposium on Two-Phase Flow Modelling and Experimentation', Pisa, 22–24 September 2004 (CD-ROM).
[27] S.S. Sazhin, W.A. Abdelghaffar, E.M. Sazhina, M.R. Heikal, Models for droplet transient heating: effects on droplet evaporation, ignition, and break-up, Int. J. Therm. Sci. 44 (2005) 610–622.
[28] A. Mukhopadhyay, D. Sanyal, A semi-analytical model for evaporating fuel droplets, ASME Journal of Heat Transfer 127 (2005) 199–203.
[29] D.J. Torres, P.J. O'Rourke, A.A. Amsden, Efficient multicomponent fuel algorithm, Combustion Theory and Modelling 7 (2003) 67–86.
[30] L.A. Dombrovsky, S.S. Sazhin, S.V. Mikhalovsky, R. Wood, M.R. Heikal, Spectral properties of diesel fuel droplets, Fuel 82 (2003) 15–22.
[31] L.A. Dombrovsky, S.S. Sazhin, Absorption of thermal radiation in a semi-transparent spherical droplet: a simplified model, Int. J. Heat Fluid Flow 24 (2003) 919–927.
[32] L.A. Dombrovsky, Absorption of thermal radiation in large semi-transparent particles at arbitrary illumination of a polydisperse system, Int. J. Heat Mass Transfer 47 (2004) 5511–5522.

[33] J.S. Chin, A.H. Lefebvre, Steady-state evaporation characteristics of hydrocarbon fuel drops, AIAA Journal 21 (1983) 1437–1443.
[34] R.W. Schrage, A Theoretical Study of Interphase Mass Transfer, Columbia University Press, New York, 1953.
[35] D.A. Labuntsov, A.P. Kryukov, Analysis of intensive evaporation and condensation, Int. J. Heat Mass Transfer 22 (1989) 989–1002.
[36] T. Ytrehus, S. Ostmo, Kinetic theory approach to interface processes, Int. J. Multiphase Flow 22 (1996) 133–155.
[37] A.P. Kryukov, V.Yu. Levashov, S.S. Sazhin, Evaporation of diesel fuel droplets: kinetic versus hydrodynamic models, Int. J. Heat Mass Transfer 47 (2004) 2541–2549.
[38] Y. Zeng, C.-F. Lee, A preferential vaporization model for multicomponent droplet and sprays, Atomization and Sprays 12 (2002) 163–186.
[39] L.A. Dombrovsky, S.S. Sazhin, A simplified non-isothermal model for droplet heating and evaporation, Int. Commun. Heat Mass Transfer 30 (2003) 787–796.
[40] S.V. Patankar, Numerical Heat Transfer and Fluid Flow, McGraw-Hill Book Company, New York, 1980.
[41] C. HirschNumerical Computation of Internal and External Flows, vol. 1, John Wiley & Sons, Chichester, 1994.
[42] H.K. Versteeg, W. Malalasekera, An Introduction to Computational Fluid Dynamics, Longman, Harlow, 1999.
[43] O.M. Todes, Quasi-stationary regimes of mass and heat transfer between a spherical body and ambient medium, in: V.A. Fedoseev (Ed.), Problems of evaporation, combustion and gas dynamics of disperse systems. Proceedings of the Sixths Conference on Evaporation, Combustion and Gas Dynamics of Disperse Systems (October 1966), Odessa: Odessa University Publishing House; 1968, pp. 151–159 (in Russian).
[44] F. Cooper, Heat transfer from a sphere to an infinite medium, Int. J. Heat Mass Transfer 20 (1977) 991–993.
[45] Z.-G. Feng, E.E. Michaelides, Unsteady heat transfer from a sphere at small Peclet numbers, Journal of Fluid Engineering 118 (1996) 96–102.
[46] S.S. Sazhin, V. Goldshtein, M.R. Heikal, A transient formulation of Newton's cooling law for spherical bodies, ASME Journal of Heat Transfer 123 (2001) 63–64.
[47] S.S. Sazhin, W.A. Abdelghaffar, S.B. Martynov, E.M. Sazhina, M.R. Heikal, P.A. Krutitskii, Transient heating and evaporation of fuel droplets: recent results and unsolved problems. In Proceedings of '5th International Symposium on Multiphase Flow, Heat Mass Transfer and Energy Conversion', Xi'an, China, 3–6 July 2005, in press.
[48] S.S. Sazhin, E.M. Sazhina, M.R. Heikal, Modelling of the gas to fuel droplets radiative exchange, Fuel 79 (2000) 1843–1852.
[49] L.A. Dombrovsky, S.S. Sazhin, E.M. Sazhina, G. Feng, M.R. Heikal, M.E.A. Bardsley, S.V. Mikhalovsky, Heating and evaporation of semi-transparent Diesel fuel droplets in the presence of thermal radiation, Fuel 80 (2001) 1535–1544.
[50] S.S. Sazhin, W.A. Abdelghaffar, E.M. Sazhina, S.V. Mikhalovsky, S.T. Meikle, C. Bai, Radiative heating of semi-transparent diesel fuel droplets, ASME Journal of Heat Transfer 126 (2004) 105–109, Erratum 126 (2004) 490–491.
[51] R.C. Ried, J.M. Prausnitz, B.E. Poling, The Properties of Gases and Liquids, McGraw-Hill Book Company, New York, 1987.
[52] P.F. Flynn, R.P. Durrett, G.L. Hunter, A.O. zur Loye, O.C. Akinyemi, J.E. Dec, C.K. Westbrook, Diesel combustion: an integrated view combining laser diagnostics, chemical kinetics, and empirical validation. SAE report 1999; 1999-01-0509.
[53] S.S. Sazhin, C. Crua, D. Kennaird, M.R. Heikal, The initial stage of fuel spray penetration, Fuel 82 (2003) 875–885.
[54] E.M. Sazhina, S.S. Sazhin, M.R. Heikal, M.E.A. Bardsley, The P-1 model for thermal radiation transfer: application to numerical modelling of combustion processes in Diesel engines, in: "Proceedings of the 16th IMACS World Congress 2000 on Scientific Computation, Applied Mathematics and Simulation" CD (paper 125-10), 2000.